2. OU 10-08 CONCEPTUAL MODEL OF GROUNDWATER FLOW

The OU 10-08 conceptual model of groundwater flow represents the current understanding of the geohydrologic features that control flow within the SRPA in the OU 10-08 study area. The two-dimensional numerical model is based on conceptual model elements. These elements, consisting of the geohydrologic framework and groundwater inflows and outflows, control the distribution of flow within the aquifer.

2.1 Geohydrologic Framework

Before describing the geology of the OU 10-08 groundwater model study area, it is necessary to briefly describe the geography and physiography of the study area, which is shown in Figure 2-1. The ESRP is a 298-km (185-mi) long, 59-km (37-mi) wide region of lowered elevation and suppressed topography surrounded by elongate Basin and Range (B&R) style mountains and valleys. The most prominent feature on the ESRP is a slightly elevated axial ridge that can be traced from Island Park in the northeast to Dietrich in the southwest. This feature, punctuated by several rhyolitic domes, including Big Southern Butte, is known as the Axial Volcanic High (AVH). Another prominent feature of the ESRP is the Great Rift of Idaho, which is an eruptive volcanic fissure complex at Craters of the Moon National Monument grading into multiple sets of Quaternary non-eruptive fissures north of Minidoka and then switching back to eruptive fissures and flows at southern edge of the rift at the Holocene Wapi Lava Field. A second volcanic rift is the Arco Rift, which extends from the town of Arco southeast past Big Southern and Cedar buttes.

The Big Lost River exits the B&R and flows onto the ESRP at Arco. Because of the elevated topography of the Arco Rift and the AVH, the Big Lost River is trapped in the Big Lost Trough (BLT), which is the prominent area of low elevation on the southern half of the INL Site. The sinks of both the Big Lost and Little Lost rivers are contained within the BLT. The sinks of Birch Creek are located at the northern edge of the BLT. Antelope and Circular buttes, just east of TAN, separate the sinks of Birch Creek from Mud Lake. The AVH forms a low ridge that separates Mud Creek from the now-almost-drained bed of Market Lake to the east. Market and Mud lakes are the remnants of a large pluvial lake, Lake Terreton, that once extended from Howe to Menan during the last glacial period.

The geohydrologic framework of the OU 10-08 study area consists of the geologic elements of the aquifer matrix. The following subsections describe the extent and boundaries of the study area, active aquifer thickness, major geologic units and hydrologic subdomains, and distribution of hydraulic properties.

2.1.1 Extent and Boundaries of the OU 10-08 Study Area

The OU 10-08 study area encompasses approximately 7,770 km^2 (3,000 mi^2) of the ESRP. This entire area is underlain by the SRPA (Figure 2-2) and extends beyond INL Site boundaries to "better accommodate regional effects and to ensure that groundwater movement beyond the [INL] boundaries can be included" (Arnett and Smith 2001). The OU 10-08 study area is bounded both by natural geohydrologic boundaries and by boundaries that have been set to most efficiently define the extent of active flow systems. These boundaries include natural boundaries to groundwater flow to the northwest, hydraulic boundaries to the southeast, and selected boundaries to the northeast and southwest.

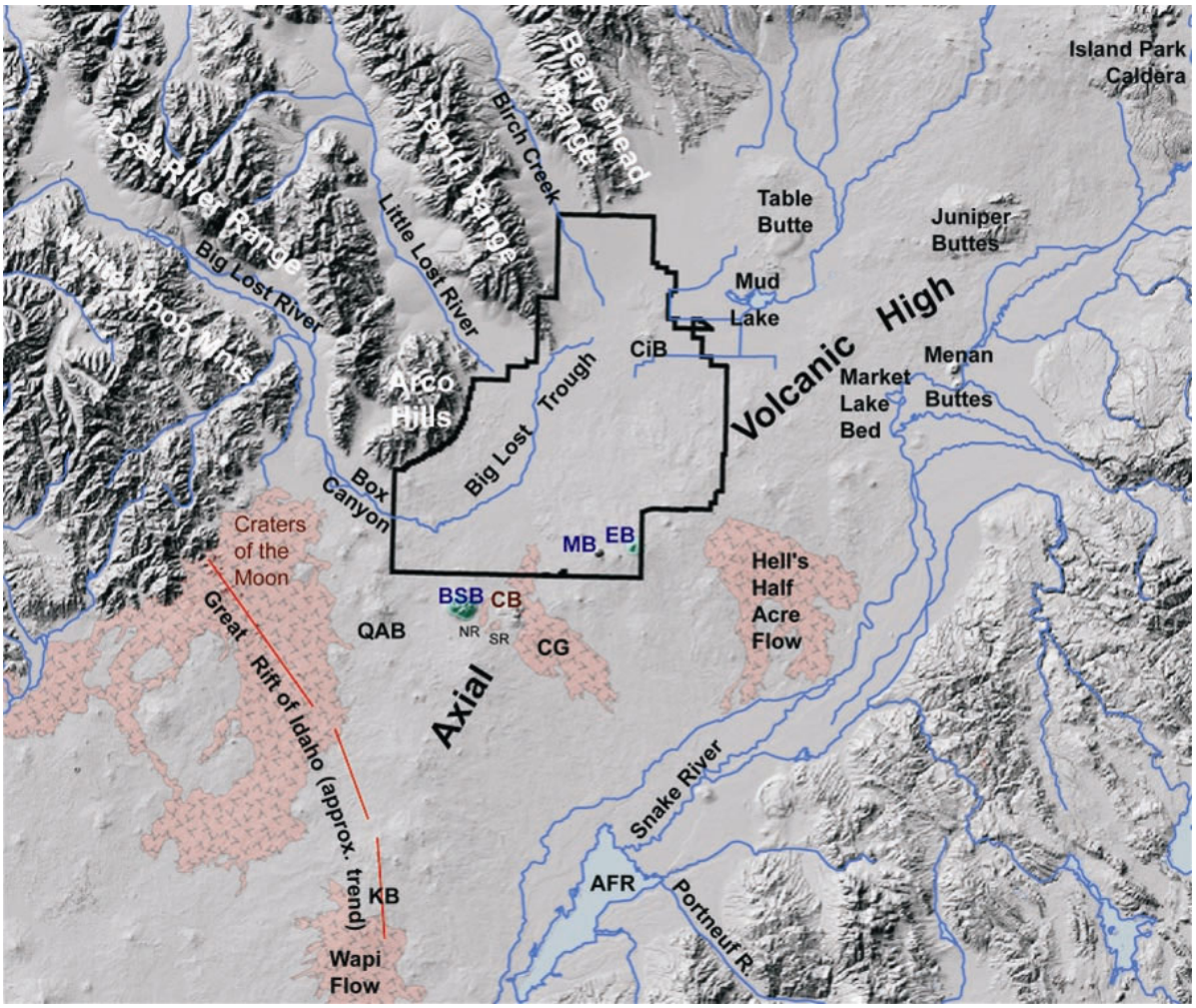

Figure 2-1. Geography and physiography of the region of the ESRP encompassing the OU 10-08 study area. (Flow and butte names in black indicate volcanic rocks that are basaltic in character, names in blue indicate volcanic rocks that are silicic in character, and names in brown indicate volcanic rocks that are intermediate in character between the pervious two types. Area abbreviations are as follows: AFR = American Falls Reservoir, BSB = Big Southern Butte, CB = Cedar Butte, CG = Cerro Grande Lava Flow, CiB = Circular Butte, EB = East Butte, KB = Kings Bowl Lava Flow and Crater, MB = Middle Butte, NR = North Robbers Lava Flow, QAB = Quaking Aspen Butte, SR = South Robbers Lava Flow.)

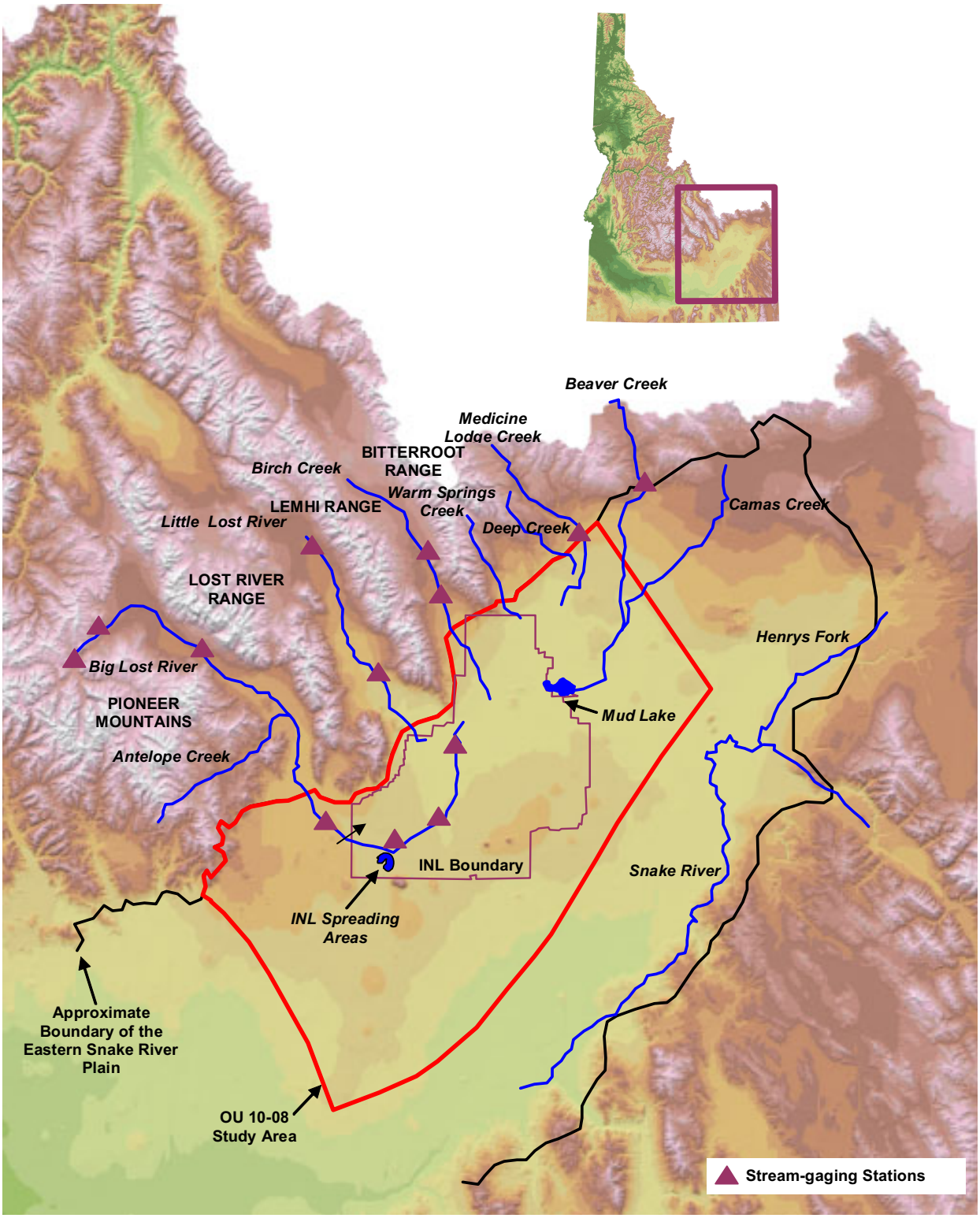

Figure 2-2. Location of the area of the ESRP represented by the OU 10-08 study area, surface-water features, and stream-gaging stations.

2.1.1.1 Northwestern Study Area Boundary. The study area is bounded on the northwest by the mountains and tributary valleys of the Bitterroot, Lemhi, Lost River, and Pioneer ranges (Figure 2-2). These B&R mountains form the northwestern edge of the ESRP. The small-permeability sedimentary rocks composing these mountains are assumed to act as a no-flow boundary to the high-permeability basalts of the SRPA. Intervening tributary drainage basins provide a source of groundwater and surface-water inflow to the SRPA.

2.1.1.2 Southeastern Study Area Boundary. The southeastern boundary of the study area (Figure 2-2) corresponds to a groundwater flow path defined by regional numerical modeling studies (Garabedian 1992; Ackerman 1995). This inferred flow path represents the general direction of flow from the northeast to the southwest and forms a hydraulic boundary across which no flow is considered to occur. This boundary was selected sufficiently distant from areas of interest to minimize the effects of this boundary on contaminant transport.

2.1.1.3 Northeastern Study Area Boundary. The northeastern boundary of the study area (Figure 2-2) is located northeast of the INL Site in the Mud Lake area. This boundary does not represent a natural geohydrologic boundary, but it was selected to provide an upgradient cross section that is perpendicular to regional groundwater underflow and sufficiently distant from the INL Site to minimize the effects of fluxes from pumpage, irrigation, and seasonal changes on groundwater flow in the area of interest. This northeast study area boundary overlaps a part of the Mud Lake area that was numerically modeled by Spinazola (1994). The location of this boundary permits comparison of simulated underflow to groundwater fluxes estimated in Spinazola's study.

2.1.1.4 Southwestern Study Area Boundary. The southwestern boundary of the study area (Figure 2-2) again does not represent a natural geohydrologic boundary. Rather, this study area boundary was selected to represent a cross section that is approximately perpendicular to groundwater flow and is sufficiently downgradient from the INL Site to accommodate known and predicted contaminant migration.

2.1.2 Active SRPA Thickness within the OU 10-08 Study Area

Representation of the geologic framework requires an understanding of the active SRPA thickness, defined as the thickness through which most groundwater flows. Most of the wells within the OU 10-08 study area are constructed only within the upper part of the aquifer and provide no direct information about the active aquifer thickness. Direct information about the active thickness is available from only eight wells that are located in the south-central part of the study area and fully penetrate the aquifer. These eight wells are INEL-1, Corehole 1, Corehole 2A, Site 14, C1A, WO-2, ANL-1, and Middle-1823.

Because most INL Site wells only penetrate the upper part of the SRPA, the thickness of basalts beneath the ESRP has been estimated primarily from electrical-resistivity geophysical data. Based on a study by Whitehead (1992, Plate 3), the estimated basalt thickness in the area represented by the OU 10-08 study area ranges from 30 m (100 ft) to more than 1,219 m (4,000 ft) thick. Lindholm (1996, p. A51) estimated that most regional groundwater flow in these basalts occurs within the upper 152 m (500 ft) of saturation.

Robertson (1974) estimated that the total aquifer system in the vicinity of the INL Site is probably more than 305 m (1,000 ft) thick, but he used a uniform thickness of 76 m (250 ft) in his numerical model to represent the upper active section of the aquifer, where most groundwater flow was believed to occur. In subsequent years, this 250-ft thickness has been widely accepted as an adequate estimate of the active thickness of the SRPA. Recent geophysical data are providing estimates of aquifer thickness that are more defensible technically.

Smith (2002) estimated the active thickness of the SRPA in the vicinity of the INL Site using a combination of direct and indirect information obtained from wells and surface geophysical surveys. The current estimates of the active aquifer thickness are derived from Smith's estimates and from recent deep corehole and temperature data. Direct evidence of the active aquifer thickness in these wells was obtained through analysis of temperature gradients, lithologic variations in drill cores, and aquifer tests (Smith 2002).

A series of temperature studies has been conducted since the 1960s to examine heat flow and structural features (Blackwell 1989 and 1990; Blackwell and Steele 1992; Blackwell et al. 1992; Olmsted 1962; Smith et al. 2001; Brott et al. 1981; and Wood and Bennecke 1994). Temperature logs from these studies provided direct information about the active thickness of the SRPA in the fully penetrating wells. The active thickness of the SRPA in the eight wells ranges from 102 m (334 ft) to 368 m (1,207 ft). The active thickness of the SRPA is characterized in these wells by nearly isothermal conditions, because the relatively fast-moving cold water in the aquifer dominates the regional geothermal gradient. Below the base of the active aquifer, the temperature profile represents the regional conductive temperature gradient.

Despite the sharp resolution of the aquifer profile obtained from any given well, the lack of deep wells across the OU 10-08 study area significantly limits the capability to establish an aquifer thickness profile across much of the INL Site. In those areas, aquifer thickness has been inferred from indirect measurements that include surface electrical-resistivity surveys and water-temperature data from shallow wells.

Two bounding estimates of thickness ("thick" and "thin") were developed for the OU 10-08 study area (Smith 2002). Both use the limited direct evidence of the aquifer base from the eight deep wells in the south-central part of the study area. The "thick" aquifer interpretation also utilizes electrical-resistivity data and water temperature at the top of the aquifer to extrapolate thickness estimates to the northeast and southwest. Colder water temperatures in those areas are correlated with assumed thicker aquifer sections, resulting in an upper bounding estimate for thickness distribution. The "thin" interpretation simply assumes a general tendency for the aquifer thickness to become gradually greater toward the center of the plain and does not utilize water-temperature information away from the area of direct evidence. Uncertainties in estimation methods and a lack of confirmatory data make it impossible to determine whether the thick or thin model best reflects actual subsurface conditions. Contour maps of the altitude of the effective base for the thick and thin interpretations are shown in Figures 2-3 and 2-4.

Cores collected from the deep wells provided additional information about the base of the active aquifer. In several wells, basalts characteristically were altered and mineralized below the depth of the temperature inflection that identifies the base. For example, Doherty et al. (1979, p. 3) observed propylitic alteration and secondary zeolite mineralization of the basalts below a depth of 488 m (1,600 ft) in well INEL-1. The capacity of underlying units to transmit water is typically considered to be orders of magnitude smaller than that of the active aquifer thickness. Aquifer tests conducted in several of the deep wells indicated that the hydraulic conductivity of rocks underlying the base of the aquifer is much smaller than that of the upper part of the aquifer. Mann (1986, p. 21) observed that the hydraulic conductivity of the upper section in the INEL-1 deep corehole (above a depth of 244 m [800 ft]) is from two to five orders of magnitude larger than that of the section below a depth of 457 m (1,500 ft). Hydraulic conductivity in the upper section ranges from 0.3 to 30 m/day (1 to 100 ft/day); hydraulic conductivity of basalts below a depth of 457 m (1,500 ft) ranges from 0.06 to 0.09 cm/day (0.002 to 0.03 ft/day). Mann (1986, p. 18) also noted a distinct change in solute chemistry between the same depth intervals.

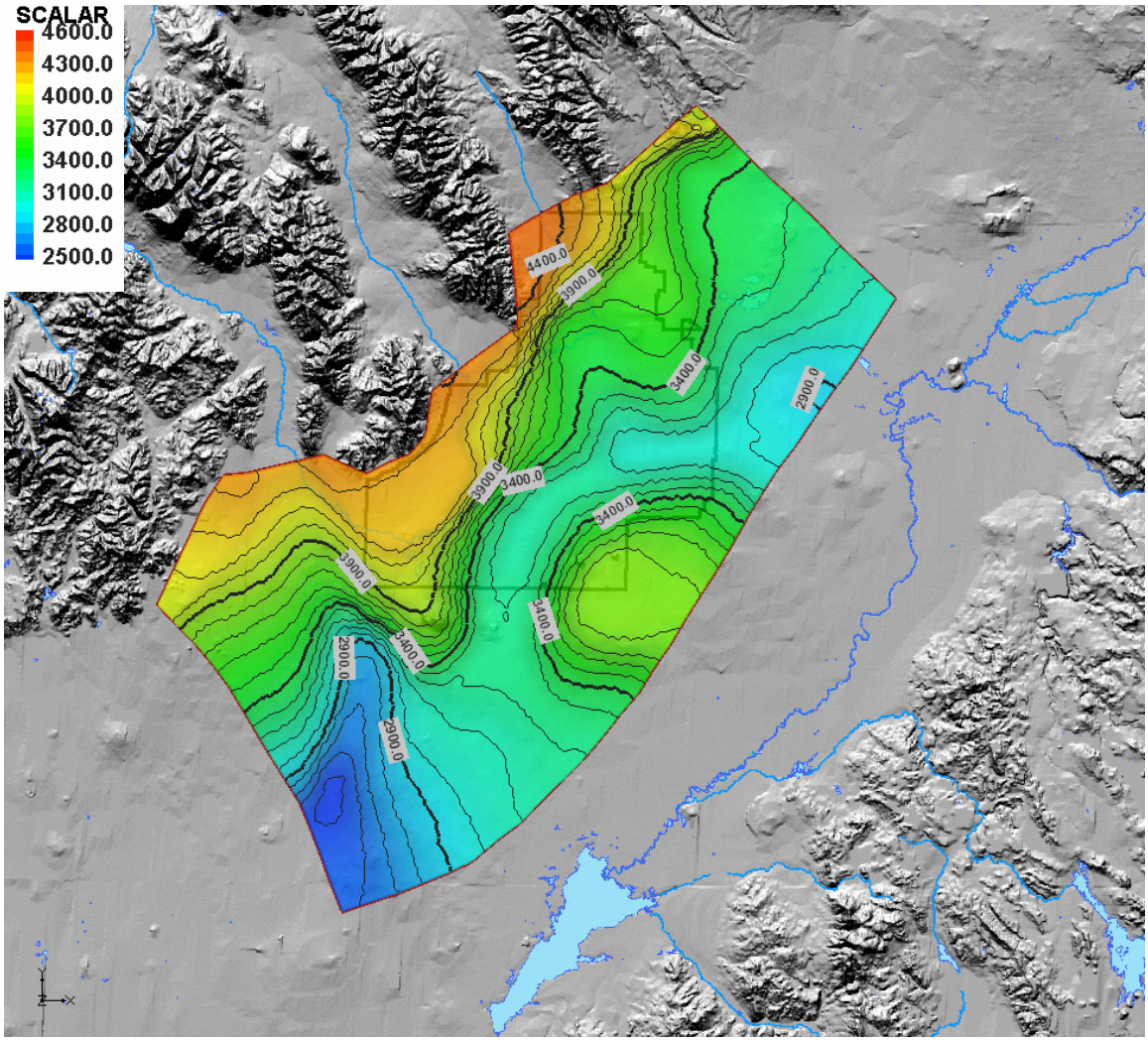

Figure 2-3. Estimated altitude of the active aquifer base in feet above sea level in the OU 10-08 study area (thick interpretation).

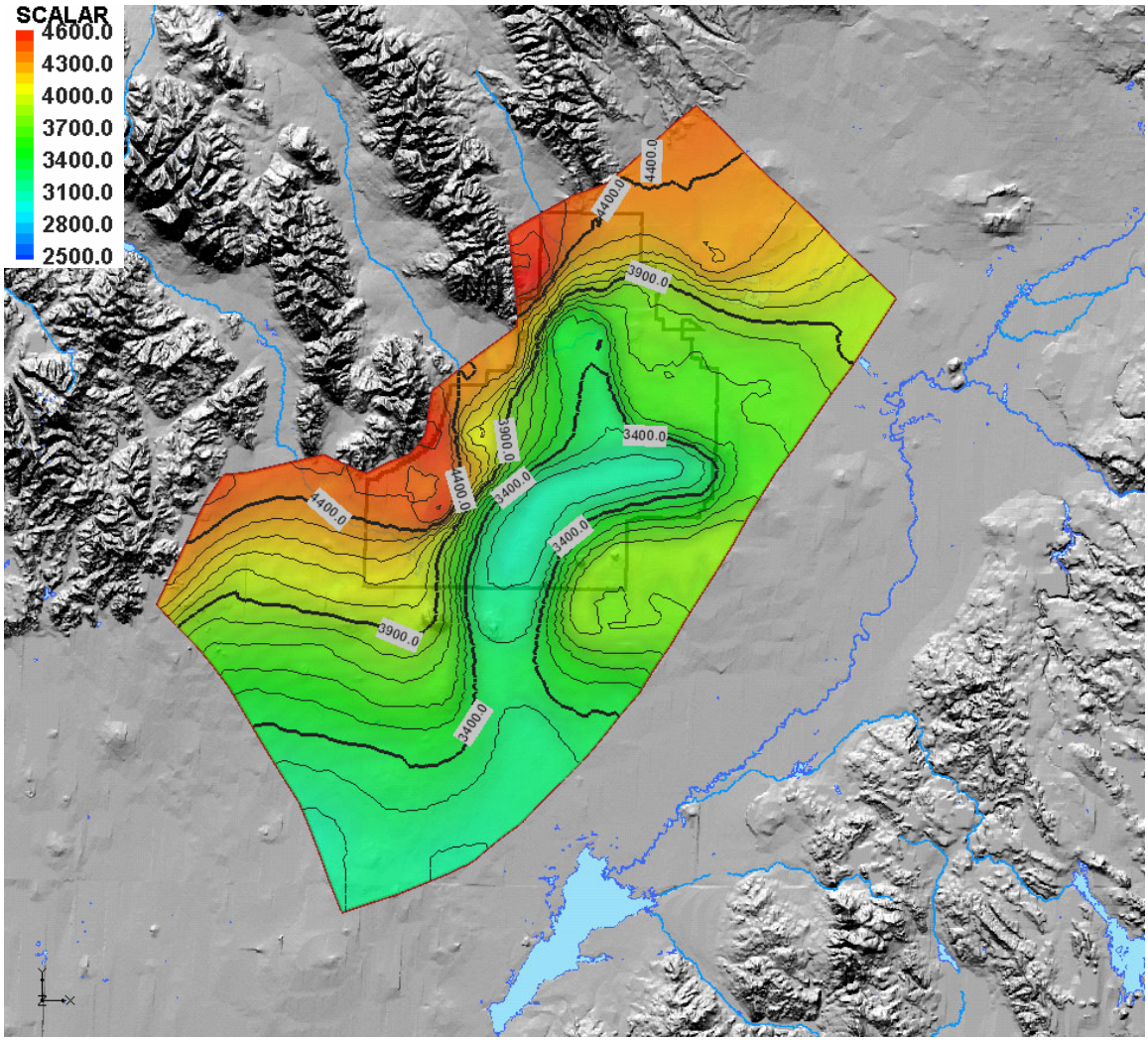

Figure 2-4. Estimated altitude of the active aquifer base in feet above sea level in the OU 10-08 study area (thin interpretation).

2.1.3 Major Geologic Units and Hydrologic Subdomains Composing the SRPA

The OU 10-08 study area can be divided into five general geologic types that consist of active volcanic rift zones, inactive volcanic rift zones, floodplains, sedimentation areas, and volcanic tablelands. These geologic types control groundwater flow by virtue of their intrinsic lithologic and stratigraphic properties.

Note that although this report describes the two-dimensional modeling effort, the division of the study area into geological units and subdomains is based on geologic features in three dimensions. While the two-dimensional model has used the surficial expression of the geologic subdomain boundaries in the construction of the model geometry, the stratigraphic nature of some of the subdomains will only be exploited to their fullest in the three-dimensional model. This caution about the three-dimensional nature of conceptual model subdomains also extends to what is shown on the location map of the subdomains. Some of the subdomains will appear to overlap when comparing their location maps; this is the simple consequence of displaying three-dimensional features in two-dimensional plan view.

2.1.3.1 Sedimentation Areas. The OU 10-08 groundwater model study area includes several areas that are mantled or interbedded with thick sequences of fine-grained sediments (Figure 2-5). There are large lakebed sequences in the north half of the study area: (a) a young pluvial sequence that is shallow and aerially exposed in places and (b) another lakebed sequence that occurs at depth and is interbedded with older basalt flows. The latter forms the top of the stratigraphic column of Subdomains 1a and 1b. The former is included in the subsurface of the volcanic tableland Subdomain 2b, as discussed in the subsections below. There is another major sediment type in Subdomain 1c of the study area, made up of a thick sequence of ponded river outwash deposits interfingered with basalt flows. These sediments are mostly fine-grained but do include some coarser sands and gravels. The three geologic subdomains where fine-grained sediments occur are described below.

Subdomains 1a and 1b - Pluvial Lakebeds—During glacial periods, pluvial lakes formed on the relatively flat ESRP, leading to widespread deposition of lacustrine sediments on top of basalt. In the northern half of the groundwater model study area, the playa deposits of Birch Creek, the Big Lost and Little Lost river sinks, and the modern Mud and Market lakes are remnants of the most recent pluvial lake known as Lake Terreton (Stearns et al. 1939). Within the study area, pluvial lakebeds are present at the surface and in the immediate subsurface stretching from Howe in the west, the Birch Creek Diversion Channel in the north, and Terreton in the east. These deposits form a thick mantle of lacustrine sediments on top of volcanic tableland basalts in much of the northern half of the study area. The base of the Lemhi Range and Lava Ridge immediately northeast of TAN divide the pluvial lakebeds and the modern river sinks at the surface into northern and southern sections. The northern section, designated as Subdomain 1a, includes Mud Lake and the sinks of Birch Creek. The southern section includes the pluvial lakebeds in the subsurface between TAN and the Naval Reactors Facility as well as the sinks of the Big Lost and Little Lost rivers. Subdomain 1b also includes a small amount of coarser-grained fluvial sediments from the Little Lost River that interfinger shallowly with both basalts and pluvial lake deposits. Under the pluvial lakebeds are thick sequences of volcanic tableland basalts with few sedimentary interbeds of mostly eolian character. The nature of volcanic tablelands is discussed in Subsection 2.1.3.2.

Subdomains 1c - Buried Inland Delta of the Big Lost River—A thick sediment mantle occurs where the Big Lost River exits the valley between the White Knob and Lost River ranges and flows onto the ESRP. The Big Lost River was captured within the BLT by the growth of the Arco Rift and the AVH. The trapping of the river caused sediment that would have originally traveled south or southwest to pond between the river's egress from the B&R and the AVH. This caused the growth of what is essentially a small inland delta that has interbedded with basalt flows erupted on the ESRP. The subsequent rise and growth of the Arco Rift, Great Rift, and other nearby eruptive centers have continued the pattern of trapping and ponding the fluvial sediment outwash at the mouth of the Arco Valley, creating an apron-shaped area where fluvial sediment and basalts interfinger and where shallow and perched B&R aquifers feed into the much deeper SRPA. This phenomenon is discussed in much greater detail in Subsection 2.2.2.4 (under the subheading Description and Location of Transition Zone Geohydrologic Features).

2.1.3.2 Volcanic Tablelands. The ESRP is an area of young volcanism. More than 99% of all volcanic rocks on the ESRP are pahoehoe-type basalt flows erupted from low-shield volcanoes, lava tubes, and fissures (see Figure 2-6). Once erupted, these basalts can travel anywhere from 0.1 km (0.6 mi) to more than 48 km (30 mi) from their eruptive vents as pahoehoe flows with an average thickness of 7 m (23 ft) (Knutson et al. 1992).

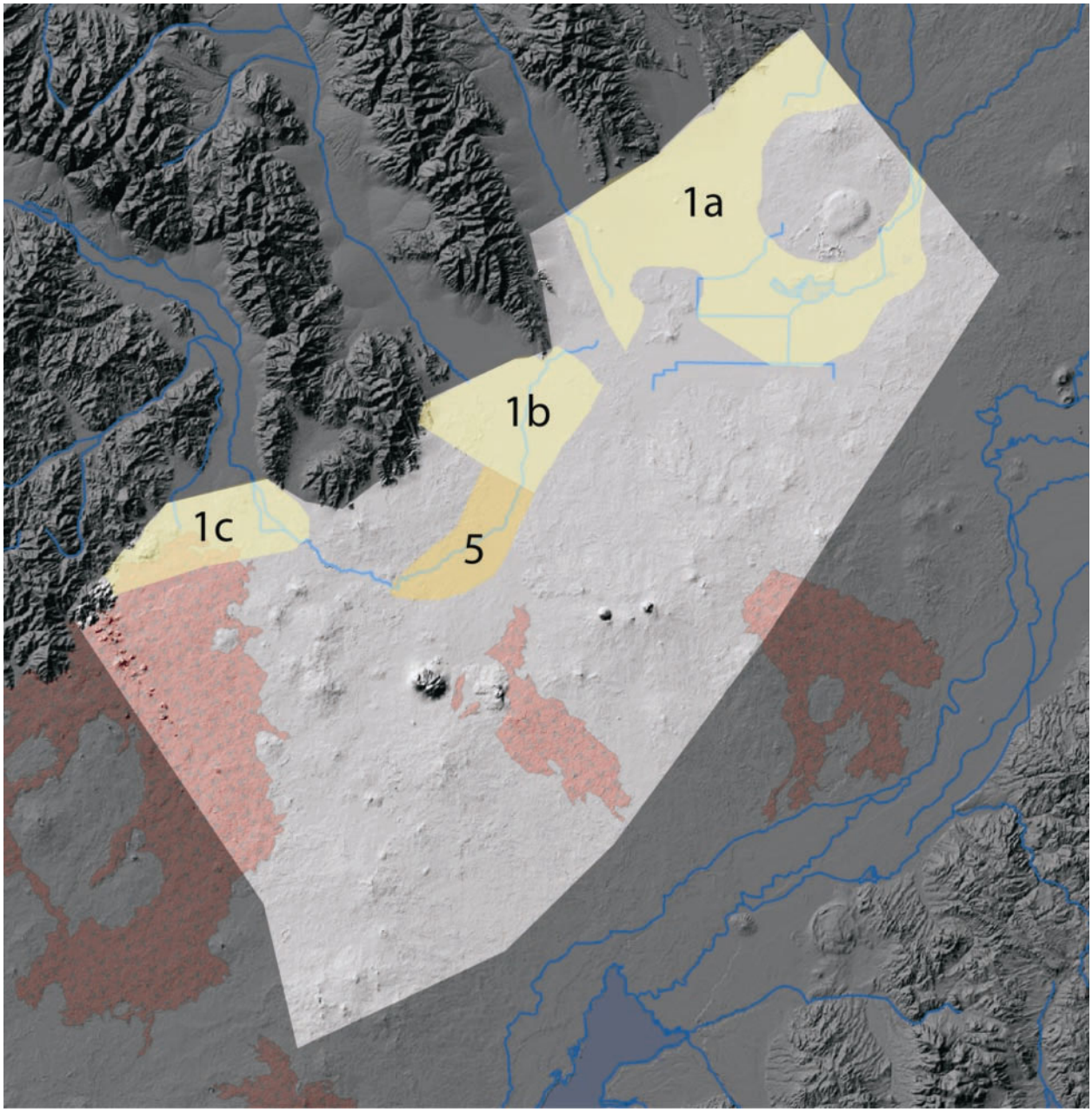

Figure 2-5. Locations of Subdomains 1a, 1b, 1c, and 5.

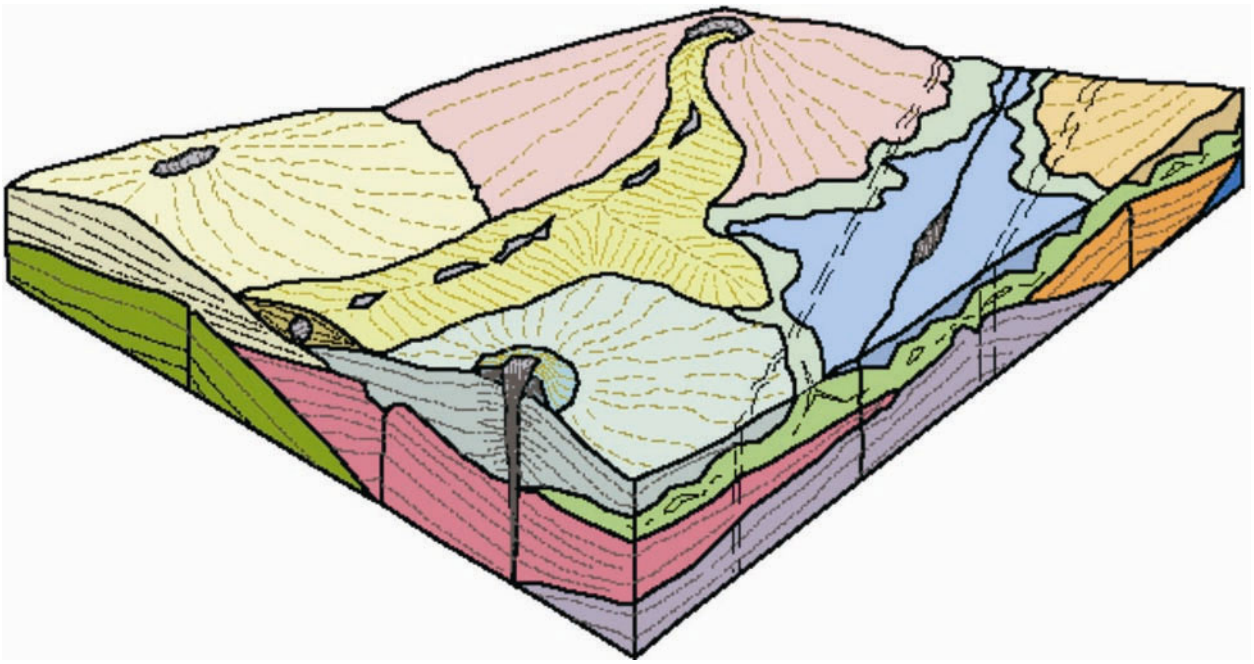

Figure 2-6. Typical ESRP pahoehoe flow eruptive styles. Basalt can erupt from fissures (shown in blue), the vents of low-angle shield volcanoes (shown in pale yellow and pale green), and vent-fed lava tubes (shown in darker yellow). The consequence of these eruptive styles coupled with the small volume of ESRP flows creates a subsurface stratigraphy that can be compared to a pile of randomly-stacked pancakes, all of different sizes (modified from Greeley [1982]).

The direction of lava flow is downhill away from vent areas. Flows stop traveling either because their vents stop feeding magma or flows become trapped within topographic lows like the BLT. Eruptive vents tend to be concentrated in areas known as volcanic rift zones such as the Great Rift of Idaho. The accumulation of these flows creates broad, mostly flat volcanic tablelands characterized by gradual topographic gradients between the elevated volcanic rift zones and the topographic lows of floodplains and sinks. The subsurface stratigraphy of the volcanic tablelands does not usually accumulate fluvial sediments, but they can include up to ~15% sedimentary materials, mostly as interbedded eolian loess. The locations of the volcanic tablelands of the conceptual model are shown in Figure 2-7.

Subdomain 2a - Table Butte Volcanic Tableland—Table Butte and the neighboring volcanoes rise above the pluvial lakebeds in the northernmost part of the study area. These basalts are all older than 700 ka. The vents of this tableland appear to be mostly in the middle of the elevated circular plateau formed by these buttes.

Subdomain 2b - West Axial Slope—This volcanic tableland was fed from vents along the AVH, with a small amount of basalt on its southern end originating from the Arco Rift. The subsurface of this tableland also includes a thick sequence of sediments named the Olduvai Lake beds (Bestland et al. 2002; Blair and Link 2000), because its age corresponds to the Olduvai normal polarity subchron of the paleomagnetic time scale, dated between 1.77 and 1.95 Ma (Cande and Kent 1995). In the extreme northern portion of the OU 10-08 study area, the Olduvai Lake sediments are shallow and above the SRPA stratigraphically. Like most other strata in the study area, however, these beds dip gradually to the south. Under TAN, the Olduvai beds intersect the SRPA. Under INTEC to the south, these beds have dipped beneath the SRPA, as shown in Figure 2-8.

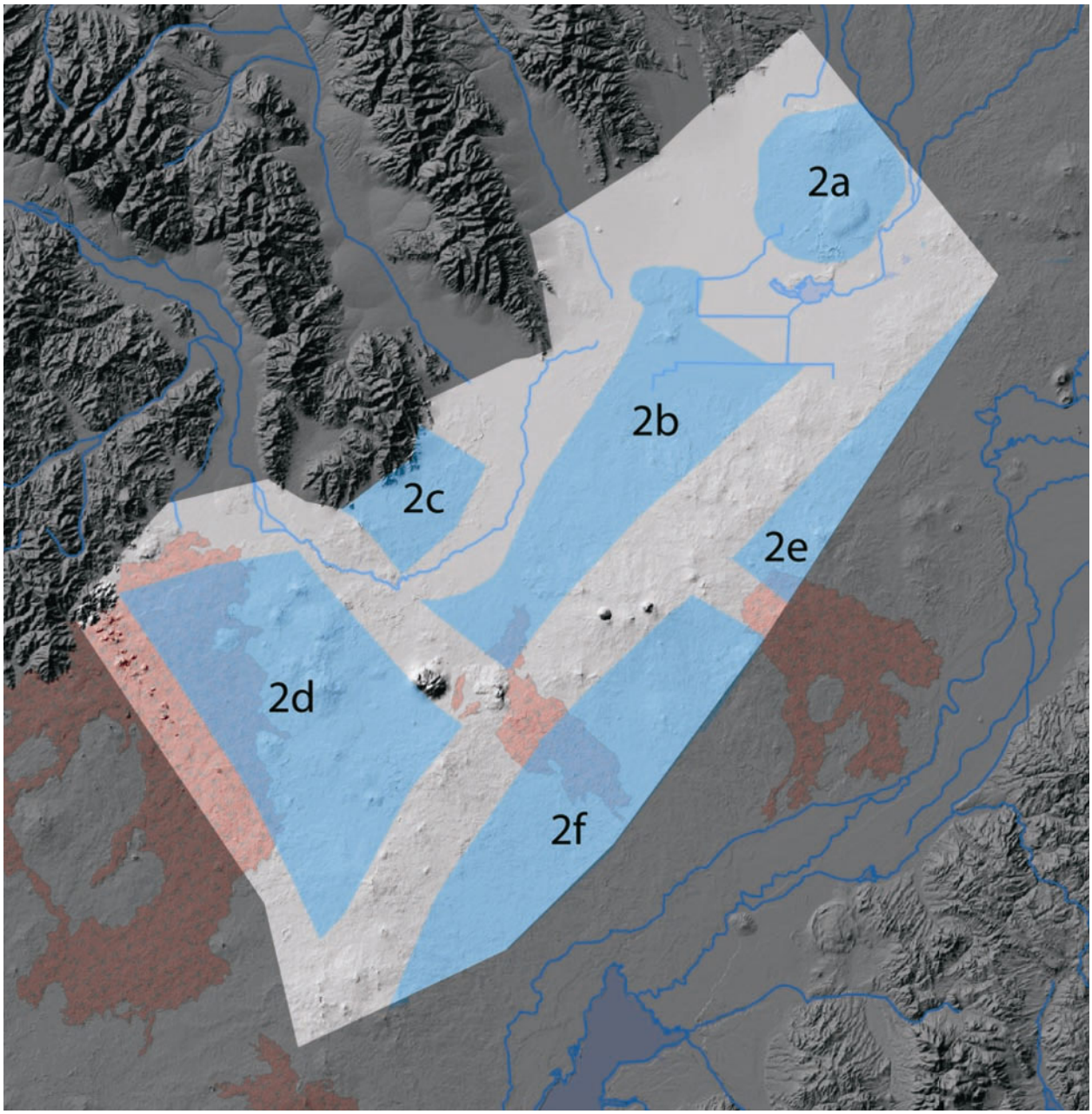

Figure 2-7. Locations of Subdomains 2a, 2b, 2c, 2d, 2e, and 2f.

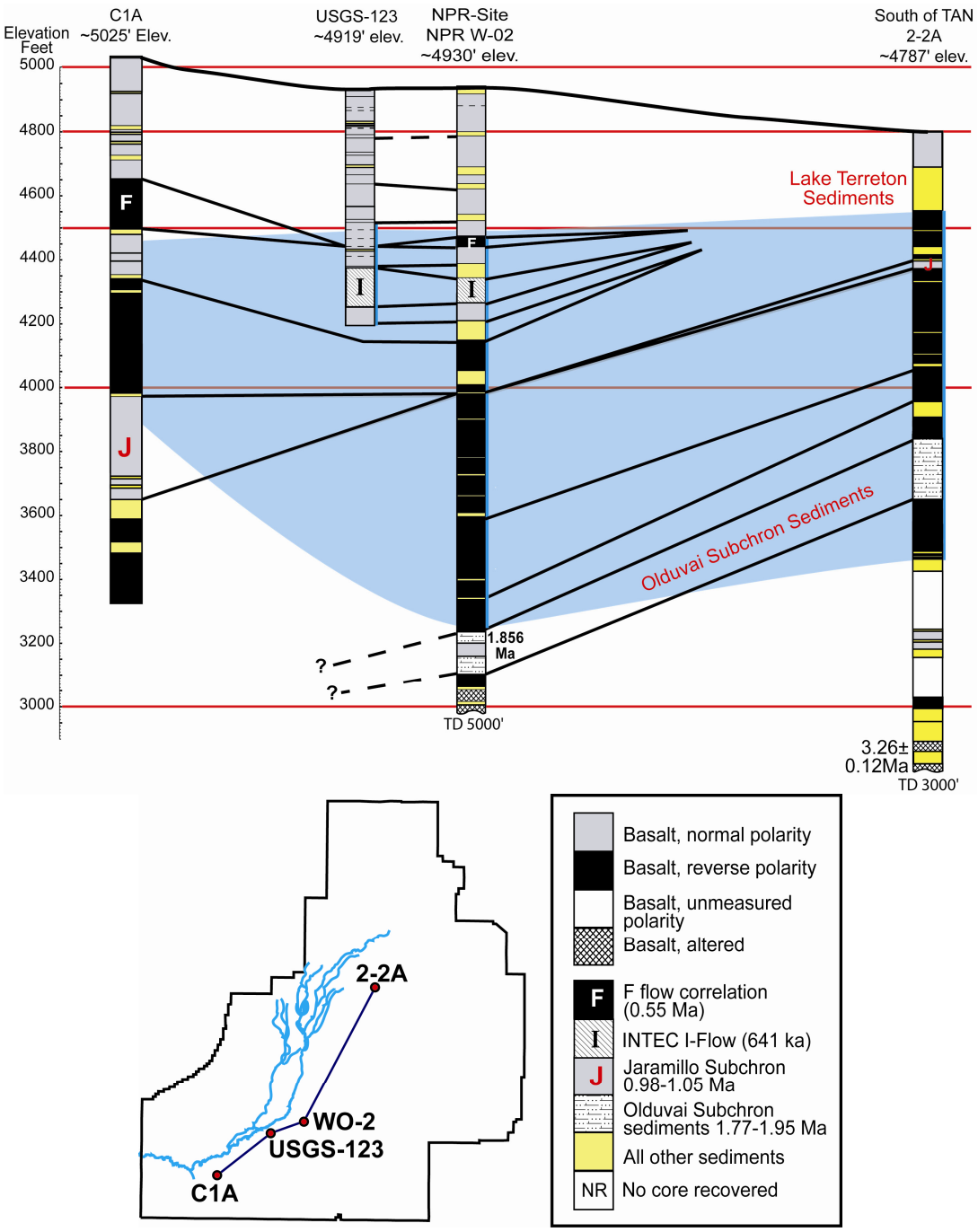

Figure 2-8. Illustration of how strata dip in a general southward direction at the INL Site in the middle of in the OU 10-08 study area. In the northern part of the study area, many flows with the oldest age dates are exposed at the surface, but in the southern part of the study area, flows of similar age are buried deep in the subsurface stratigraphy. In a similar manner, the approximately 2-million-year-old Olduvai Lake sediments are within the active SRPA flows on the north end of the INL Site and dip to the south so that they are underneath the SRPA in the south-central part of the INL Site. Flows and interbeds with radiometric age dates of approximately a half a million years old or less (the "F-flow" stratum) dip in an upward fashion from the center of the INL Site toward the southwest corner of the site; this is due to uplift of the Arco Rift, which has elevated an area that stretches from the town of Arco to the vents of the Cerro Grande Lava Field southeast of Big Southern Butte. The normal-polarity stratum shown in pink are hypothesized to be flows of Jaramillo Subchron age, based on a new radiometric age date for basalt core from well C1A just north of the RWMC (Helm-Clark and Rodgers 2004).

Subdomain 2c - Crater Butte Volcanic Tableland—The basalts of this tableland originated from Crater Butte and other Arco Rift vents or from the now inactive and mostly buried AEC Butte Rift. Along its western boundary, the basalts of this tableland interfinger with floodplain deposits of the Big Lost River. There is a thick sequence of sediments deep in the subsurface of this subdomain, but this sequence occurs below the base of the aquifer and, therefore, has no affect on groundwater flow.

Subdomain 2d - Quaking Aspen Butte Volcanic Tableland—This subdomain includes all of the tableland basalts between the Great Rift and the Arco Rift. The postulated Quaking Aspen Butte Rift runs through the center of this tableland. Because it lies within the loci of three active or recent rift features, this tableland is higher than all other volcanic tablelands on the ESRP. Its altitude leaves it more exposed to wind and wildfire, the two processes that act together to strip vegetation and prevent soil formation and sediment accumulation. As a result, the sediment-to-basalt ratio is lower here compared to other tablelands, less than 10% versus less than 15% elsewhere. Because of its proximity to three volcanic rifts, the amount of cinder and ash in the subsurface is higher than elsewhere.

Subdomains 2e and 2f - Southeast and Northeast Axial Slope—The volcanic tablelands east of the AVH receive more precipitation than the volcanic tablelands west of the AVH, which are in the rain shadow of the mountains to the northwest of the study area. Volcanic tablelands on the east side of the ESRP are also within the watershed of the Snake River, which provides more water and deposits more sediment than the rivers that feed the BLT. The volcanic tablelands on the east side of the ESRP may, therefore, have slightly more interbedded sediment in the subsurface as one approaches the Snake River. The tableland of the east slope of the AVH is divided in two, where the dividing line coincides with the non-eruptive fissures and elongated vent of the Hell's Half Acre Lava Field and Rift feature. Basalts north of this line originate from the AVH or from the nexus of volcanic vents centered on Butterfly and Kettle buttes west of Idaho Falls, just outside of the study area. Tableland basalts south of the Hell's Half Acre line originate from the AVH or from off-axis vents like Taber Butte.

2.1.3.3 Active Volcanic Rift Zones. The earth science community has not agreed on the number and exact character of volcanic rifts on the ESRP. Consequently, the geologic conceptual model for the SWGM restricts itself to rift features whose existence is beyond doubt or rift features that are known or suspected to have an influence of groundwater flow, most likely because rifts concentrate relatively low-permeability volcanic rocks like cinder and ash.

Within the study area, features are further divided into active rifts and older, inactive rifts. Active volcanic rifts on the ESRP share several distinguishing features: elevated topography, lines of vents and/or fissures (> 0.9 km [> 0.6 mi]) whose surface expression can be mapped, and surface evidence of Holocene and latest Pleistocene volcanism (< 20,000 years). The four features within the study area that satisfy these criteria are described below. The locations of active volcanic rifts are shown in Figure 2-9.

Subdomain 3a - Axial Volcanic High—The AVH is the largest, highest, and longest feature on the ESRP. Quaternary and latest Pleistocene volcanism occurs where the AVH intersects other active rift systems. Unlike other rift systems, however, the AVH is aligned roughly parallel to the general direction of groundwater flow in the SRPA. In terms of stratigraphy, the eruptive rocks of the AVH are derived from small basaltic vents and from large rhyolitic laccoliths like Big Southern Butte that are fed by small feeder dikes. The off-axis rocks of the AVH are mostly volcanic tableland basalts with one big difference: higher heat flow under the AVH. The AVH within the study area has a higher heat flux than its surroundings, resulting in a thicker transition between the aquifer and the subaquifer zone, which is an example of three-dimensional features that are not easily accommodated by two-dimensional modeling. The base of the SRPA is controlled by the horizon between fresh and altered basalts, where the altered basalt has lost all porosity due to the growth of authigenic and alteration minerals (Morse and McCurry 2002). The alteration of subsurface basalts is driven by temperature. Along the AVH where heat flux is higher, the transition from fresh basalt to porous-clogged altered basalt will be thicker compared to cooler areas such as the BLT.

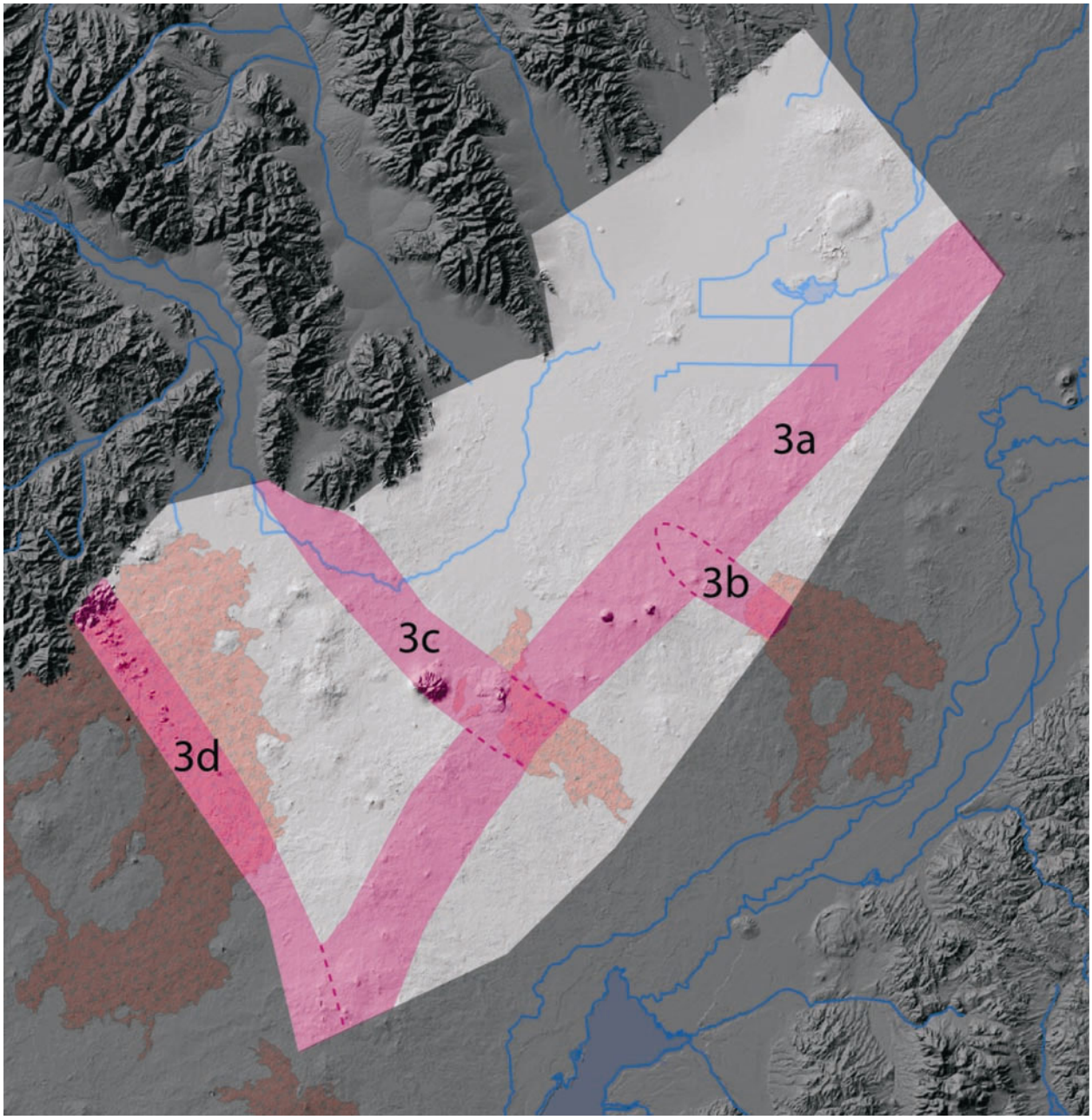

Figure 2-9. Locations of Subdomains 3a, 3b, 3c, and 3d.

Subdomain 3b – Hell's Half Acre Rift—The Hell's Half Acre Rift feature begins just off the axis of the AVH, where two sets of non-eruptive northwest-southeast trending fissures can be observed at the surface, disrupting a thin loess cover and ~350-ka basalts, from the edge of the lava field to almost as far as Route 20, 3 km (1.9 mi) away. Approximately 6 km (3.7 mi) to the southeast and in line with the fissure sets is the 0.9-km (0.6-mi) long linear crater that forms the vent of the 5.1-ka Hell's Half Acre lava flow.

Subdomain 3c - Arco Rift—The Arco Rift is a feature that is approximately 4 km (2.5 mi) wide. Its active portion is between the late Pleistocene Arco flow, west of the town of Arco, and the vents of the 13.4-ka Cerro Grand Lava Field south of Atomic City. The oldest dated feature along the Arco Rift is

Cedar Butte at ~400 ka. Between the 12-ka North and South Robbers flows and the Arco flow are several non-eruptive Quaternary fissures and vertical normal faults, two of which control the path of the Big Lost River through Box Canyon. The inactive extension of the rift along its southeasterly trend intersects Ferry Butte along the Snake River and Buckskin Butte south of Blackfoot.

Subdomain 3d - Great Rift of Idaho—The Great Rift of Idaho has already been described in the first paragraph of Subsection 2.1. Within the context of the groundwater model, the portion of the Great Rift within the Craters of the Moon National Monument forms part of the southwest boundary of the model domain.

2.1.3.4 Older Inactive Volcanic Rift Zones. Older inactive rifts included in the geologic conceptual model must meet two criteria. First, the rift feature must appear to affect local groundwater flow. Second, firm geologic evidence must exist in the subsurface to support the existence of the rift—for example, a line of volcanic vents surrounded by basalt flows or a sequence of scoria cones logged in core. Currently, the three features that meet these criteria are Lava Ridge, the AEC Butte Rift, and the Quaking Aspen Butte Rift (Figure 2-10).

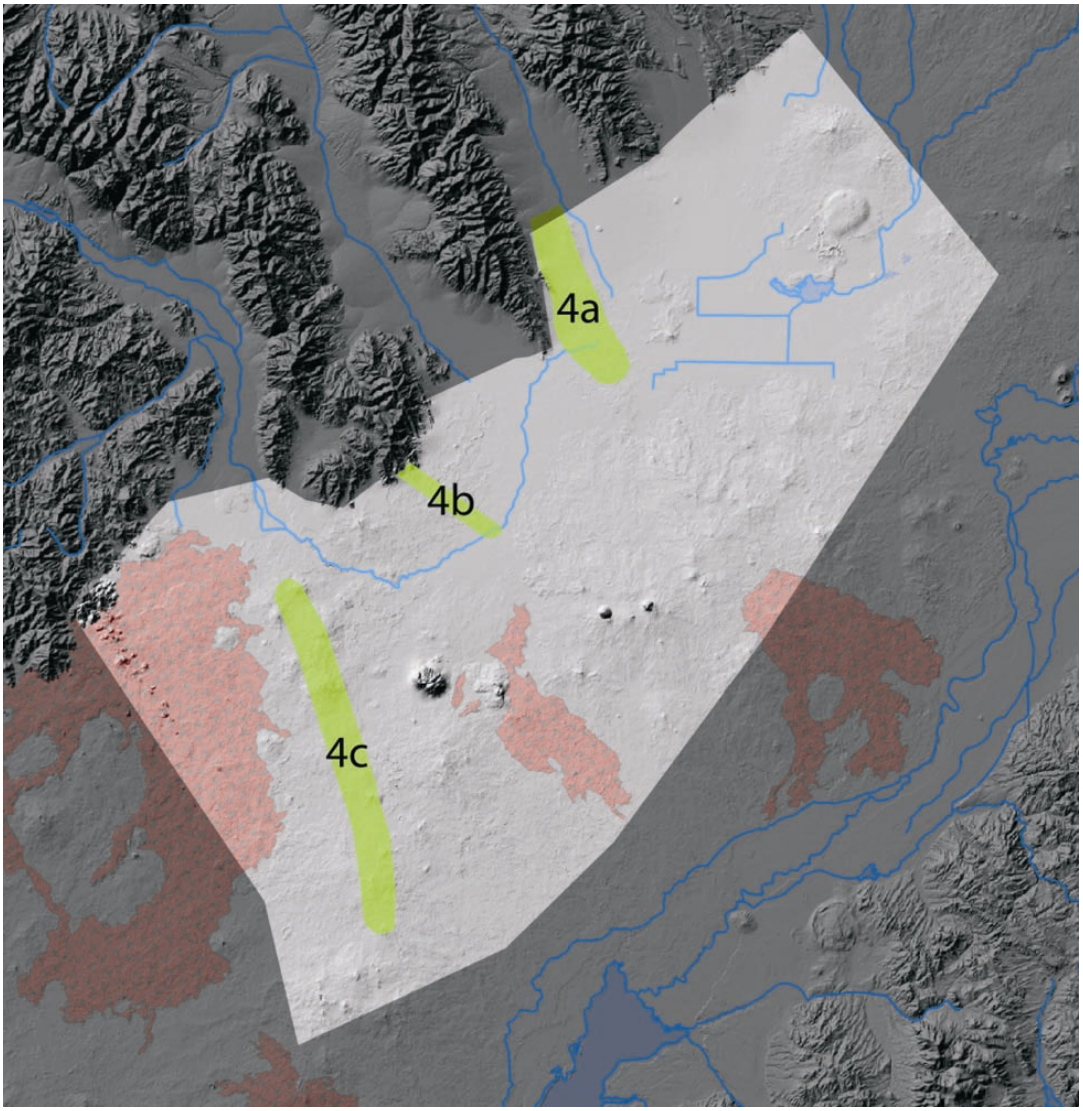

Figure 2-10. Locations of Subdomains 4a, 4b, and 4c.

Subdomain 4a - Lava Ridge—Lava Ridge is formed by a 8-km (5-mi) long line of shield volcanoes with ages between ~800 ka and ~1 Ma. The linear feature appears to influence the local flow of groundwater northeast of TAN.

Subdomains 4b - AEC Butte Rift—The surface expression of the AEC Butte Rift is a line of three volcanic vents, including the 626-ka AEC Butte itself immediately northwest of the RTC. The rift extends across the floodplain of the Big Lost River to INTEC, where scoria and other near vent facies occur at ~90 m (~300 ft) below land surface at the INTEC tank farm.[b] The thickness and dip of flows at the RTC also indicate that a vent or vents existed to the east of the floodplain between 640 and 350 ka (Helm-Clark et al. 2004). This rift feature might be the cause of a zone of lower transmissivity at INTEC and north of the RTC (Anderson et al. 1999).

Subdomain 4c - Quaking Aspen Butte Rift—The Quaking Aspen Butte Rift is a linear feature made up of shield volcanoes, many of which date between 40 and 64 ka. This line of vents extends from Wildhorse Butte on its north end to Mosby Butte in the south. This feature might account for the possible upflow, low-transmissivity feature responsible for the low water-level measurement at the Site-2 well in the tableland between the Arco Rift and the Great Rift.

2.1.3.5 Floodplain of the Big Lost River. Geologically, the floodplain of the Big Lost River, Subdomain 5 (see Figure 2-5), is the most complex portion of the study area, where meandering braided fluvium interfingers with pahoehoe basalts originating from several different volcanic rift zones surrounding the BLT. Sediments and basalt flows have deposited in the floodplain coming from three different directions, making a very complex stratigraphic column in the subsurface under the path of the river (Figure 2-11). An additional complication is the fact that basalt flows entering the floodplain area from the west and southwest are 61 to 122 m (200 to 400 ft) higher in elevation than flows of equivalent age that enter the floodplain area from the AVH to the east and southeast.

2.1.4 Distribution of Hydraulic Properties

A detailed literature search was performed to locate and identify aquifer test information on the ESRP in the vicinity of the study area. Ackerman (1991) summarized 183 aquifer tests conducted in 94 wells from the early 1950s to the early 1990s. Since that time, a large number of tests have been conducted in support of cleanup activities at INL Site facilities. Many of these tests are documented in INL Site reports, IWRRI reports, and engineering design files. In a number of cases, however, only a summary table (with no test data for review) could be located in correspondence control files in the INL Site archives.

A total of 306 tests were identified in 182 wells, inclusive of those reported by Ackerman (1991). Of these, 48 were multiple-well tests (with each observation well data set considered individually), 204 were single-well tests, 33 were packer tests, 13 were slug tests, seven were injection tests, and one was a recovery test. Most of these tests were conducted on the INL Site, with the tests being sparse near the boundaries of the study area and in the southwest portion of the study area. Specific capacity data from a number of wells in the Idaho Department of Water Resources well completion database were used to augment the data set to include measurements outside of the INL Site boundary. These data were generally from irrigation wells along the southeast boundary of the study area. The locations of wells with aquifer test data are shown on Figure 2-12. Table A-1 in Appendix A summarizes the test information, such as the discharge rate and duration, drawdown, calculated transmissivity, and analysis method. Most of the tests were analyzed using the regression method presented by Ackerman (1991), but type curve matching methods, such as the Theis (1935) or Neuman (1972) methods, were used whenever possible.

---

b. Catherine M. Helm-Clark, unpublished sampling log, Idaho National Laboratory, November 2004.

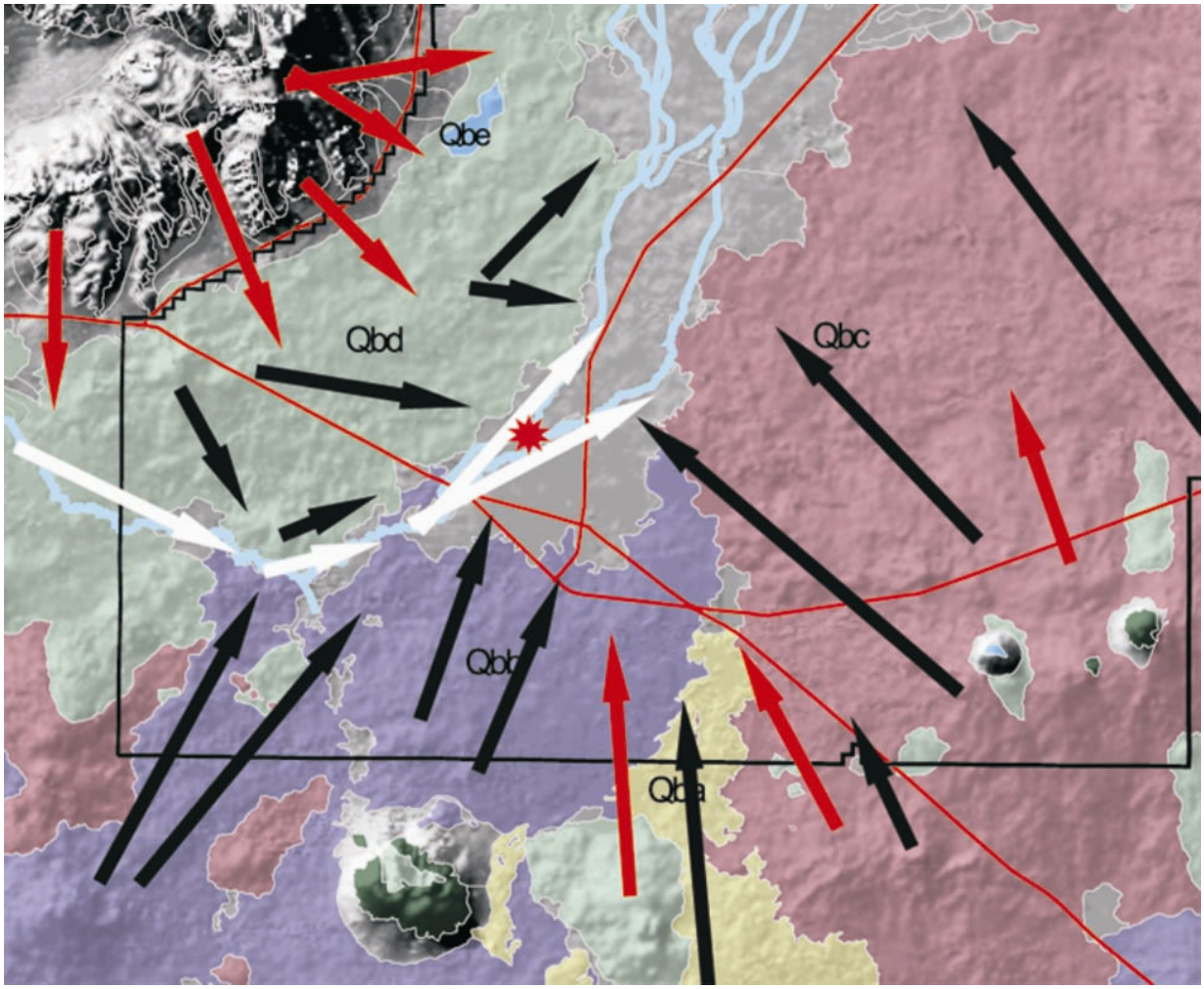

Figure 2-11. Travel directions of basalt flows and sediments into the floodplain of the Big Lost River. The red lines represent major roads, and the thin black line represents a portion of the INL Site boundary. White arrows show the path of fluvium. Red arrows show the path of alluvial materials. Black arrows show the travel paths of basalt flows simplified from Kuntz et al. (1994). The geologic unit symbols for basalts are the same as those from the most recent geologic map of the INL Site from Kuntz et al. (1994).

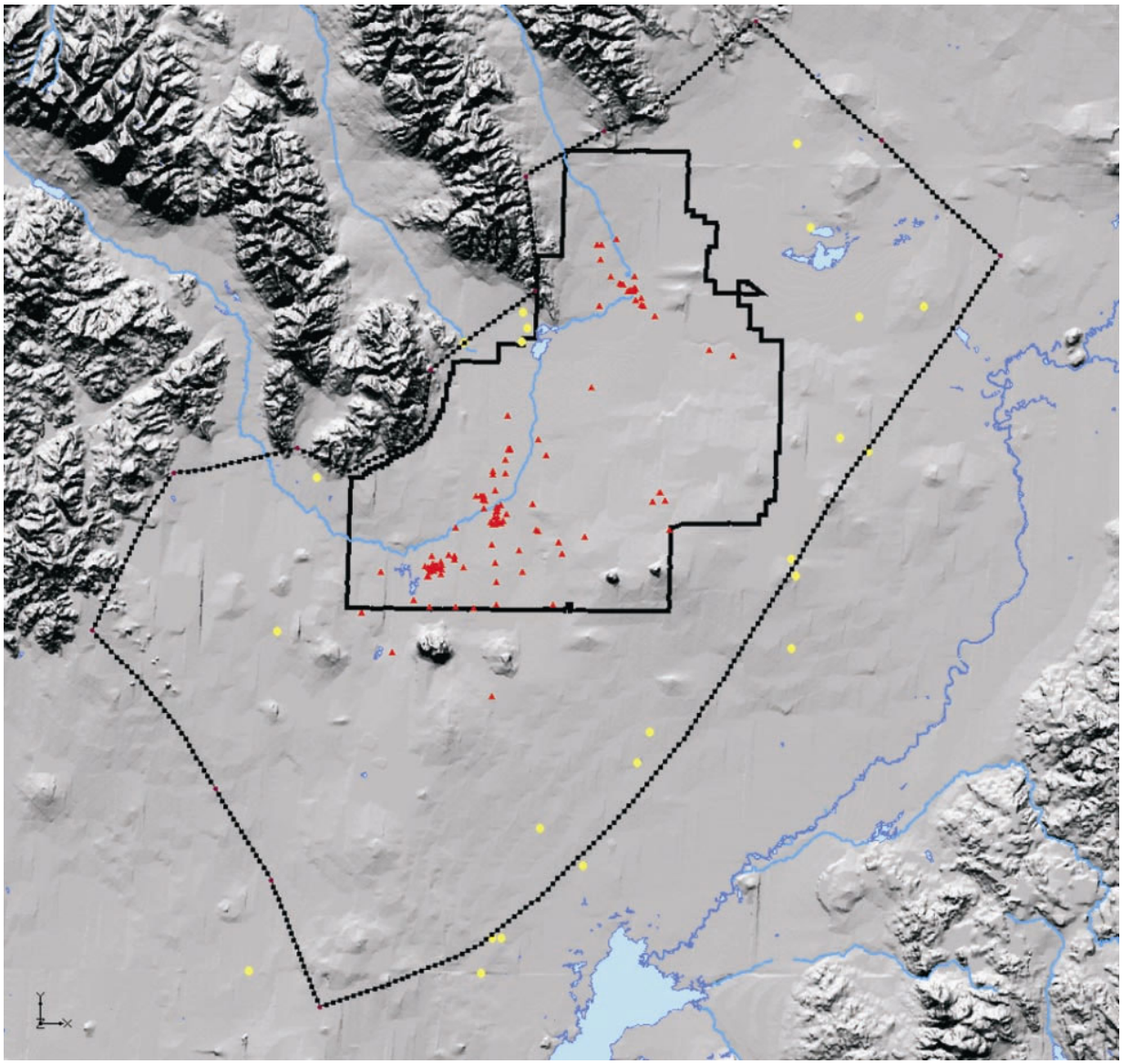

Figure 2-12. Well locations where aquifer test data are available. Red dots indicate INL Site or USGS well locations with aquifer test data. Yellow dots indicate irrigation wells with specific capacity data from the Idaho Department of Water Resources database that are used to augment the data set in areas of sparse aquifer test data.

Many of the wells on the INL Site have been tested numerous times. The oldest production wells (those drilled in the 1950s) have had as many as six aquifer tests. The test data from the wells with multiple tests were evaluated in order to assign a representative transmissivity value. Three basic variables were evaluated: the test time, the pumping rate, and the method used for the original aquifer test analysis. In general, tests with higher pumping rates and longer duration, and those analyzed with curve matching techniques, were found to be more representative in estimating aquifer parameters. This analysis is focused on preparing hydraulic property distributions for the two-dimensional model, so depth-specific packer tests, which evaluated only a small portion of the aquifer at low flow rates, were not used. These data will be used at a later date with the three-dimensional model.

Table A-2 in Appendix A summarizes the representative hydraulic conductivity and well completion information for the wells listed in Table A-1. Because the wells only partially penetrate the active portion of the aquifer, the hydraulic conductivity was calculated using laminar horizontal flow and assuming that the open interval of the well was the aquifer thickness. While this assumption will likely result in conservatively high estimates of the hydraulic conductivity, it allows for testing the various aquifer thickness scenarios using the numerical model. The hydraulic conductivity distribution over the study area is also shown graphically in Figure 2-13. In total, data from 146 wells were used to prepare the hydraulic conductivity distribution for the two-dimensional model. The calculated hydraulic conductivity ranged over seven orders of magnitude, with a mean value of 9.8×10^2 m/day (32×10^2 ft/day) and a range from 5.0×10^{-3} to 3.5×10^4 m/day (16.4×10^{-3} to 11.5×10^4 ft/day). This range equates to values representative of dense basalts and loess to highly fractured basalts, interbeds, and coarse gravels (Freeze and Cherry 1979). Figure 2-14 shows a histogram of the hydraulic conductivity values, where a nearly log-normal distribution can be seen.

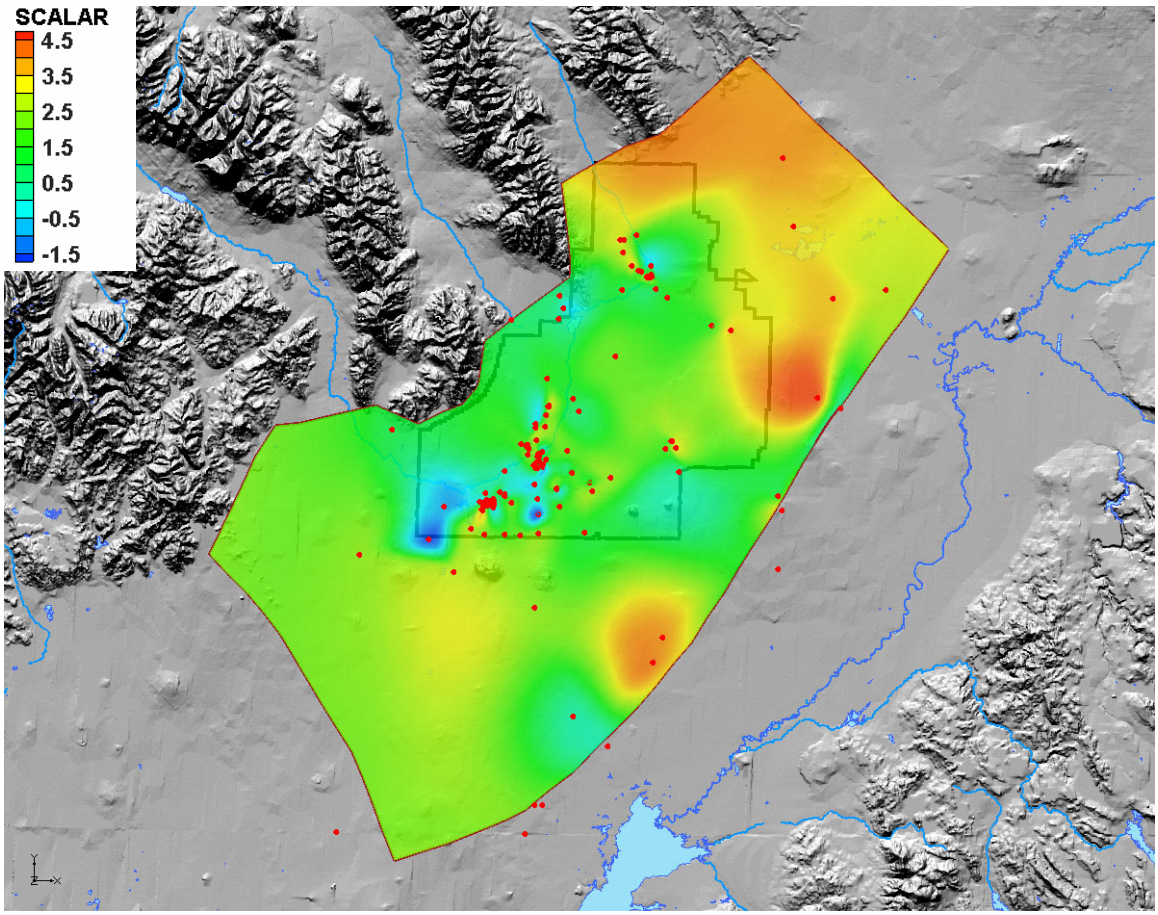

Figure 2-13. Hydraulic conductivity distribution of the study area. Red dots indicate well locations with aquifer test data. Shown is the log-transformed hydraulic conductivity in m/day.

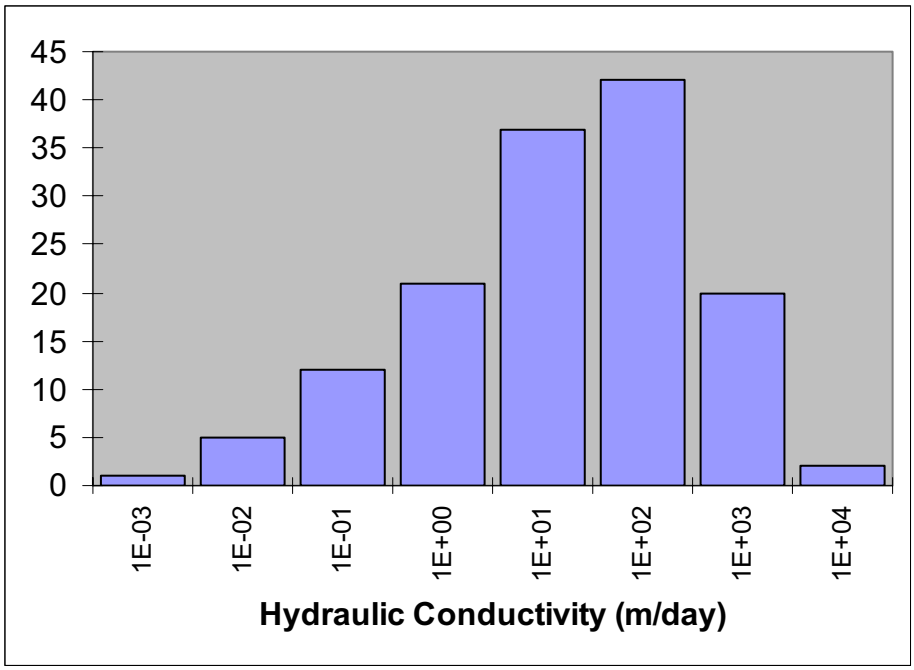

Figure 2-14. Distribution of the hydraulic conductivity binned on the logarithmic scale.

The aquifer test data were also evaluated based on the geologic subdomains presented in Subsection 2.1.3. Figure 2-15 shows the geologic subdomains overlain on the aquifer test location map. A number of subdomains, including all of the inactive rift zones and the subdomain at the mouth of the Big Lost River drainage, had no aquifer tests. Most of the aquifer tests were completed in the floodplain of the Big Lost River (Zone 5) and the volcanic tablelands in the central part of the INL Site (Zone 2b). These zones contain the major facilities on the INL Site and have been studied in the greatest detail. Table 2-1 summarizes the number of aquifer tests conducted in each subdomain and the range in hydraulic conductivity.

2.2 Inflows and Outflows

Major inflows to the SRPA within the OU 10-08 study area consist of regional underflow across the northeastern study area boundary, inflows derived from tributary basin underflow and streamflow, and recharge from infiltration of areal precipitation. Outflows occur as regional underflow across the southwestern study area boundary. Table 2-2 summarizes the water budget for the OU 10-08 study area. Values in this subsection represent annual averages for use in the two-dimensional steady-state flow model.

2.2.1 Regional Underflow into the OU 10-08 Study Area

Regional underflow enters the OU 10-08 study area from the Mud Lake area northeast of the INL Site. This regional underflow is derived from recharge of runoff from the Yellowstone Plateau to the northeast and from tributary basin inflows north of the INL Site. Groundwater flow in the Mud Lake area is characterized by extensive groundwater development for agricultural uses and by significant interaction between groundwater flow systems and surface-water features such as the Henry's Fork and its associated canal systems. This complex hydrologic system is marked by seasonally changing groundwater levels and distinct vertical hydraulic gradients within the SRPA.

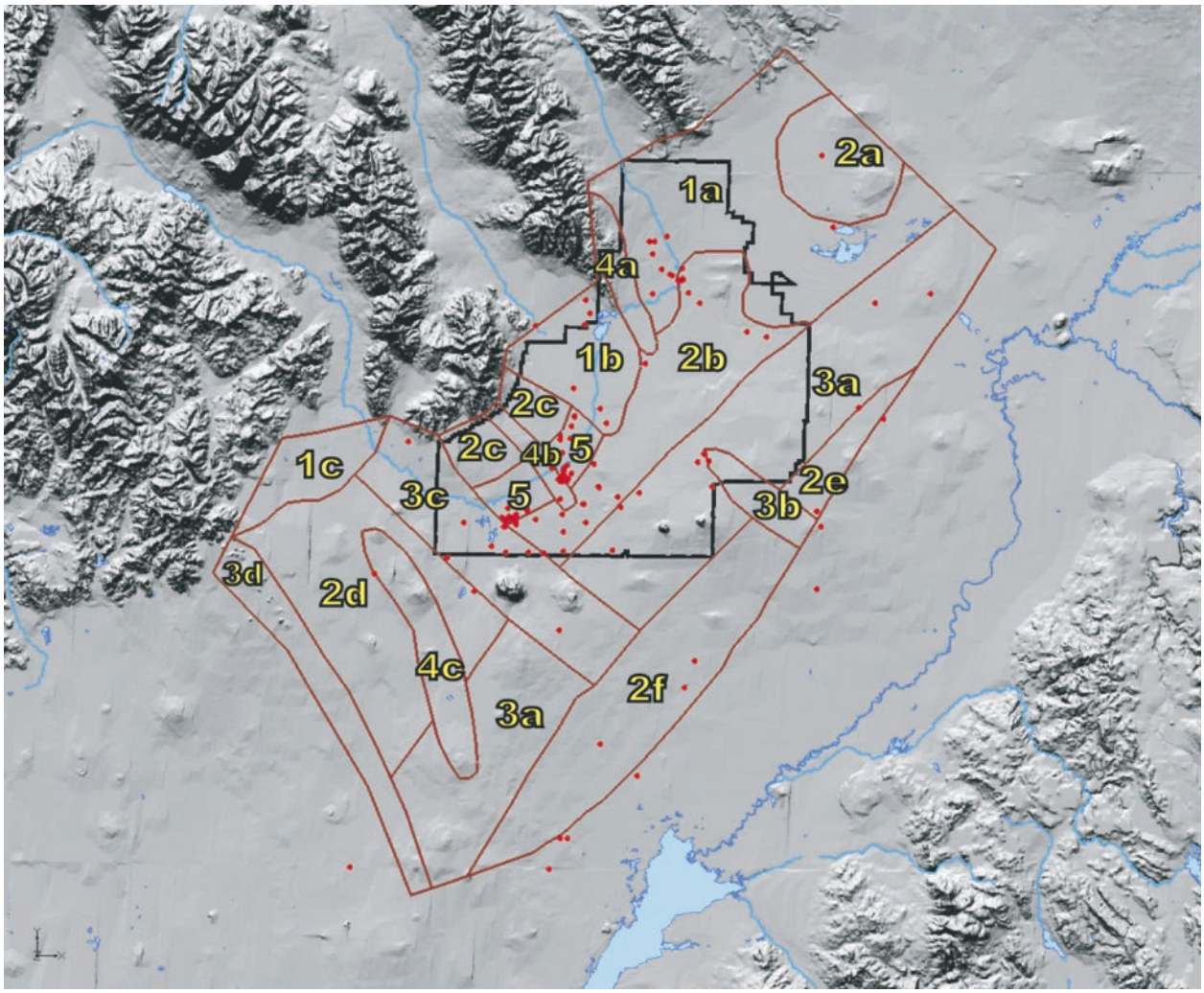

Figure 2-15. Map of the study area showing the distribution of aquifer tests within each subdomain.

Table 2-1. Subdomain hydraulic conductivity distribution.

Subdomain Number	Description	Number of Aquifer Tests	Hydraulic Conductivity Range (ft/day)	Hydraulic Conductivity Range (m/day)
Sedimentation Areas				
1a	Pluvial Lakebed	10	4.6E+01 to 8.8E+03	1.4E+01 to 2.7E+03
1b	Pluvial Lakebed	7	1.6E+00 to 1.6E+02	5.0E-01 to 4.9E+01
1c	Buried Inland Delta of the Big Lost River	0	Not applicable	Not applicable
Volcanic Tablelands				
2a	Table Butte Volcanic Tableland	1	2.9E+04 to 2.9E+04	8.8E+03 to 8.8E+03
2b	West Axial Slope	37	9.8E-01 to 9.6E+03	3.0E-01 to 2.9E+03
2c	Crater Butte Volcanic Tableland	1	3.6E+01 to 3.6E+01	1.1E+01 to 1.1E+01
2d	Quaking Aspen Butte Volcanic Tableland	2	8.1E+02 to 2.2E+03	2.5E+02 to 6.8E+02
2e	Northeast Axial Slope	4	8.5E-00 to 1.2E+05	2.6E+00 to 3.5E+04
2f	Southeast Axial Slope	8	5.6E+00 to 4.1E+01	1.7E+00 to 1.3E+01
Active Rift Zones				
3a	Axial Volcanic High	9	1.0E+01 to 1.2E+04	3.2E+00 to 3.6E+03
3b	Hell's Half Acre Rift	1	5.6E+03 to 5.6E+03	1.7E+03 to 1.7E+03
3c	Arco Rift	10	7.9E-02 to 1.9E+04	2.4E-02 to 5.9E+03
3d	Great Rift of Idaho	1	5.1E+02 to 5.1E+02	1.6E+02 to 1.6E+02
Inactive Rift Zones				
4a	Lava Ridge	0	Not applicable	Not applicable
4b	AEC Butte Rift	0	Not applicable	Not applicable
4c	Quaking Aspen Butte Rift	0	Not applicable	Not applicable
Big Lost River Floodplain				
5	Big Lost River Floodplain	55	1.6E-01 to 2.9E+04	5.0E-02 to 8.7E+03

Table 2-2. Sources of inflow and outflow for the OU 10-08 study area.

	cfs	acre-ft/yr	m^3/day
Inflows			
Regional underflow (Spinazola [1994] outflow minus Kjelstrom [1986] estimates of underflow from Medicine Lodge, Warm Springs, Deep, and Birch creeks[a])	1,105	799,993	2,703,799
Spinazola regional underflow minus Medicine Lodge, Warm Springs, Deep, and Birch creeks[a]	1,124	813,739	2,750,257
Medicine Lodge Creek	13	9,412	31,809
Warm Springs and Deep Creeks	42	30,407	102,768
Birch Creek underflow/streamflow[b]	108[b]	78,188	264,260
Little Lost River underflow/streamflow[b]	214[b]	154,929	523,625
Big Lost River underflow[b]	408[b]	295,379	998,314
Big Lost River streamflow	97	70,255	237,344
Areal precipitation (2%)	35	25,339	85,640
Areal precipitation (5%)	88	63,709	215,323
Outflows			
Underflow out of the OU 10-08 study area (2% precipitation)	2,022	1,463,871	4,947,559
Underflow out of the OU 10-08 study area (5% precipitation)	2,075	1,502,241	5,077,242

a. Spinazola's (1994) underflow of 1,268 cfs included inflow from Medicine Lodge, Warm Springs, Deep, and Birch creeks. His estimate also included areal precipitation recharge in the area of overlap, not subtracted here.
b. Kjelstrom's (1986) estimates of underflow from the tributary basins are presented here. Underflows added to the two-dimensional model from the Birch Creek, Little Lost River, and Big Lost River tributary basins were 102, 227, and 361 cfs, respectively, as derived from USGS preliminary models and within the uncertainties identified by Arnett and Smith (2001).
cfs = cubic feet per second

Spinazola (1994) constructed a numerical model to evaluate the consequences of increased development and reduced recharge on future water supplies in the Mud Lake area. The southwestern boundary of this numerical model overlaps the northeastern end of the OU 10-08 study area. Estimated underflow across Spinazola's southwest boundary is 1,268 cubic feet per second (cfs) (918,000 acre-ft) annually and includes water contributed to the system from the tributary basins to the northeast of the INL Site (Birch, Deep, Warm Springs, and Medicine Lodge creeks) and from direct precipitation in the study area overlap.

2.2.2 Inflows from Underflow and Streamflow in Major Drainage Basins Tributary to the Eastern Snake River Plain

The ESRP is bounded on the northwest by mountains and valleys of the B&R Province. This mountainous region forms a sequence of drainage basins that are tributary to the plain. Tributary basins contributing flow to the northwestern edge of the OU 10-08 study area include the Birch Creek, Little Lost River, and Big Lost River basins (Figure 2-2). Basins also include Medicine Lodge, Deep, and Warm Springs creeks to the northeast of the INL Site.

2.2.2.1 Tributary Basins to the Northeast of the INL Site. Medicine Lodge, Deep, and Warm Springs creeks drain tributary basins in the Centennial Mountains at the northern end of the ESRP. These drainages contribute streamflow and underflow to the regional flow system.

Kjelstrom (1986) used basin regression techniques to estimate underflow from these tributary basins (Table 2-1). Underflow from Medicine Lodge Creek was estimated to be 13 cfs (9,412 acre-ft/year). Combined underflow from Deep and Warm Springs creeks was estimated to be 42 cfs (30,407 acre-ft/year).

2.2.2.2 Birch Creek Tributary Basin. Birch Creek drains a tributary basin of more than 1,036 km^2 (400 mi^2) that includes the mountains of the Lemhi and Bitterroot ranges and the intervening Birch Creek Valley. Streamflow in Birch Creek is sustained by discharge from springs and seeps where bedrock intersects the land surface.

A USGS gaging station was maintained seasonally on Birch Creek near the Reno Ranch from 1967 until 1987. Daily discharges for the period of record ranged from about 40 cfs to more than 80 cfs. The average annual discharge for 1967 and 1987 ranged from 56 to 62 cfs. Based on this intermittent record, streamflows in Birch Creek are relatively constant and probably represent groundwater discharge from tributary basin aquifers. All flows in Birch Creek are diverted to a ditch near the point of entry onto the ESRP. This ditch transports water east to the Reno Ranch and is used in power generation and irrigation upgradient from the INL Site.

Water derived from watershed runoff infiltrates the alluvial deposits filling the Birch Creek Valley and moves downgradient toward the intersection with the ESRP. Underflow within these deposits provides a source of inflow to the aquifer.

Kjelstrom (1986) used basin-yield equations to calculate an average annual rate of groundwater flow of 108 cfs (78,188 acre-ft/year) through these alluvial deposits. Garabedian (1992) used this underflow rate as a source of groundwater inflow to the SRPA. Spinazola (1994) estimated similar rates for underflow and streamflow from the Birch Creek tributary basin, varying rates annually based on water levels in an index well. He used a variable inflow based on a formula that calculated a single underflow and estimated monthly underflows using water levels in an index well.

2.2.2.3 Little Lost River Tributary Basin. The Little Lost River drains an area of about 2,494 km^2 (963 mi^2) of mountainous tributary basin (Swanson et al. 2002) that includes the northeastern slopes of the Lost River Range and the western slopes of the Lemhi Range (Figure 2-2). Most tributaries to the Little Lost River infiltrate before reaching the river and do not contribute significantly to streamflow.

Streamflows were monitored from 1941 through 1989 at a gaging station on the Little Lost River approximately 11 km (7 mi) upstream from Howe. Average annual discharge during this period was 77 cfs, ranging from 49 to 107 cfs. Downstream from this gaging station, most streamflows are diverted for irrigation or infiltrate. Streamflow contributions to inflow to the SRPA are considered to be inconsequential.

Kjelstrom (1986) used basin-yield equations to calculate an average annual rate of groundwater flow of 214 cfs (154,929 acre-ft/year) through the alluvial deposits of the Little Lost River tributary basin. Garabedian (1992) used this underflow rate as a source of groundwater inflow to the SRPA. Recharge likely takes place in a transitional area at the mouth of the Little Lost River Valley as downward leakage from perched systems derived from tributary basin underflow to the aquifer below.